Entrainment of Air by a Solid Surface Plunging into a Non-Newtonian Liquid

Olivier Cohu and Hadj Benkreira
Dept. of Chemical Engineering, University of Bradford, West Yorkshire, BD7 1DP, United Kingdom

An experimental investigation of the effect of fluid rheology on air entrainment in plunging tape experiments (dip coating) was carried out. The critical velocity at which the dynamic wetting line breaks up, allowing air to entrain into the liquid, was measured for a range of viscoelastic polymer solutions in glycerin/water mixtures. Variations of the critical velocities with various solutions were found to be unexpectedly small in comparison with the large viscosity variations. The results suggest that dynamic wetting failure and subsequent air entrainment are governed by nonhydrodynamic phenomena occurring at the molecular scale at the wetting line. It was also found that fluid elasticity gives rise to flow instabilities that may lead to a different, hydrodynamic mechanism of air entrainment.

Introduction

Air entrainment is a major limitation of many industrial processes, examples of which include coating operations where a thin liquid film is applied onto a continuous solid substrate such as in the manufacturing of photographic films, magnetic tapes, adhesive strips, and wall paper. Such coating operations all involve a dynamic wetting process whereby air in contact with a dry substrate is displaced by a liquid. At low substrate speeds, the liquid wets the solid completely but as the speed is increased above a certain threshold, wetting failure occurs and air is entrained between the liquid and the solid. Air bubbles may remain attached to the substrate, creating defects on the coated product, or may detach into the coating solution, creating other problems such as stabilized emulsion or foam formation. In both cases, the product quality is affected so that production rates are eventually limited by the onset of air entrainment.

The study of air entrainment in coating flows has largely been based on dip-coating experiments where a smooth flat substrate is plunged into a large pool of stagnant liquid, as shown in Figure 1. The angle formed at the plunging point by the free surface of the liquid and the substrate and measured through the liquid is termed the dynamic contact angle (Figure 1). It increases steadily with the substrate speed until it approaches 180° at a critical velocity V_{ae} where air begins to entrain into the liquid. Previous studies focusing on this simple flow situation have helped to describe certain general features (see Burley, 1992 for review). Buonopane et al. (1986) showed that the wettability of the solid surface has little effect on the air entrainment velocity which depends mainly on the properties of the liquid, namely viscosity. With Newtonian liquids and various smooth plastic substrates, Burley and Jolly (1984) observed experimentally that the air entrainment velocity V_{ae} correlates with the liquid properties as

$$V_{ae} \approx 70.5\left[\mu\left(\frac{g}{\rho\sigma}\right)^{0.5}\right]^{-0.77} \quad \text{(in c.g.s. units)}. \qquad (1)$$

Equation 1 also fits the data of others workers (Burley and

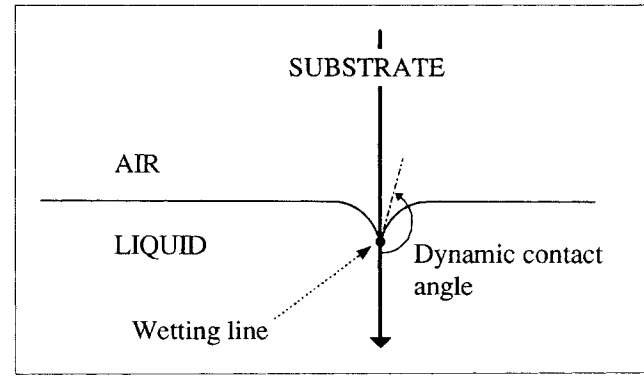

Figure 1. Dip-coating (plunging tape) experiment.

Correspondence concerning this article should be addressed to H. Benkreira.
Current address of O. Cohu: Ilford Imaging GmbH, 1705 Fribourg, Switzerland.

Kennedy, 1976; Gutoff and Kendrick, 1982; Burley, 1992; Cohu and Benkreira, 1998). Here g is the acceleration of gravity, and μ, σ, and ρ are the viscosity, the surface tension, and the density of the liquid, respectively. Dip-coating experiments have also allowed the mechanism of air entrainment to be investigated. Above a first critical velocity $V_{dwf} \leq V_{ae}$ dynamic wetting failure occurs. The wetting line suddenly becomes unstable and breaks up into a sawteeth pattern where a thin air layer, triangular in shape, penetrates between the liquid and the solid surface (Deryagin and Levi, 1964; O'Connell, 1989; Veverka, 1995). Blake and Ruschak (1979) attributed this behavior to the existence, for a given gas/liquid/solid system, of a maximum speed of wetting. They observed that the wetting line breaks up so that the component of the substrate speed normal to each individual segment does not exceed the maximum wetting speed. Further experimental evidence of this has been given recently by Cohu and Benkreira (1998). Increasing the substrate speed above V_{dwf} eventually leads to the entrainment of visible air bubbles into the liquid, due to instability of the air/liquid interface of the triangular air pockets (Severtson and Aidun, 1996). Though the speed interval $\Delta V = V_{ae} - V_{dwf}$, where V_{ae} is the critical velocity and where *visible* air bubbles entrain into the liquid, is probably finite (Veverka and Aidun, 1998), it is usually very small so that both V_{dwf} and V_{ae} may often be confounded in practice.

Virtually all previous studies of air entrainment in dip-coating were concerned with Newtonian liquids. However, industrial coating liquids nearly always contain dissolved polymers and/or suspended particles and as a result are usually non-Newtonian. Bolton and Middleman (1980) included some viscoelastic solutions to their experimental investigation of air entrainment in a single-roll coating system. Their experimental setup consisted of a rotating roller half-immersed into a bath of liquid, but the surface of the roller was not scraped prior to re-entering the bath. Air entrainment, therefore, occurred at a liquid/liquid juncture and did not result from dynamic wetting failure but rather from purely hydrodynamic instability. In this flow situation, they found that fluid elasticity postpones air entrainment to much higher speeds. Higher air entrainment velocities in dip and slide coating (with dry substrates) were also reported by Gutoff and Kendrick (1982, 1987) with a polyvinyl alcohol solution and by Blake and Ruschak (1997) with shear-thinning aqueous gelatin. Unfortunately, very few data were shown and no rheological data were made available by these authors. Also, their conclusions that air entrainment with non-Newtonian liquids occurs at higher speeds compared to Newtonian liquids of the same viscosity is controversial since the viscosity of non-Newtonian liquids is usually not uniquely defined but shear-rate dependent.

Recently, Ghannam and Esmail (1997) presented an experimental investigation of dynamic wetting of fibers that included five non-Newtonian polymeric solutions; however, air entrainment data were given for only three of them. They used dimensional analysis to work out a characteristic shear rate of the wetting problem as

$$\dot{\gamma}_a = V/L \tag{2}$$

where V is the substrate speed and L is the capillary rise

$$L = (\sigma/\rho g)^{1/2}, \tag{3}$$

and characterized non-Newtonian liquids with their viscosity at this particular shear rate. On this basis, they found air entrainment velocities to be higher with non-Newtonian liquids compared to Newtonian liquids of the same viscosity at the characteristic shear rate. Unfortunately, the significance of this result is difficult to assess, for the basis of comparison between non-Newtonian and Newtonian liquids—the characteristic shear rate—was chosen for mathematical convenience and hardly rests on physical arguments. In any case, the limited number of available data do not allow the influence of liquid rheology on the air entrainment velocity in coating operations to be assessed conclusively. Hence, there is the need for further experiments.

In the present study, air entrainment velocity measurements obtained on a laboratory-scale dip-coater with a range of non-Newtonian liquids are presented. The purpose is to investigate experimentally whether and how air entrainment is affected by non-Newtonian characteristics of the liquid. In particular, attempts are made to distinguish the effect of fluid elasticity—which was not taken into account in the analysis of Ghannam and Esmail (1997)—from that of shear-thinning. Overall, this article aims to generate a first inventory of air entrainment experimental data with non-Newtonian liquids.

Experimental Studies

The experimental setup is depicted in Figure 2. A 50-mm-wide vertical polypropylene tape was drawn downwards through a Perspex tank containing the liquid. The dimensions of the tank were $150 \times 135 \times 90$ mm [height (h) $\times$ depth ($2d$) $\times$ width (w)]. The tape passed over grounded metal rollers to reduce any static charges (Burley and Jolly, 1984), plunged into the liquid, emerged from a narrow slit at the bottom of the tank, and was finally wound around a cylinder driven by a variable speed motor. This simple design prevented the fluid carried along the substrate at the exit of the pool from flowing back and entraining air bubbles into the tank. Another advantage was that the bulk flow of the liquid within the tank on either side of the tape far from its edges was a well-defined free-surface side-driven cavity flow. The aspect ratio of the cavity a_c is defined as the tape-to-wall distance (d), divided by the liquid height (H) (that is, $a_c = d/H$, see Figure 2). Although the liquid height H was allowed to change during the experiments, as some liquid was entrained out of the pool by the substrate, the aspect ratio was always kept between 0.6 and 1.6 and it was checked that the results were insensitive to changes in a_c within this range.

The tape velocities were measured with a portable digital tachometer targeted on an idler roller. The onset of dynamic wetting failure V_{dwf} was determined by slowly increasing the tape velocity until the breakup of the wetting line into a sawteeth pattern could be observed with the naked eye under proper illumination. At this point, air bubbles were almost always entrained into the liquid. In other words, both critical velocities V_{dwf} and V_{ae} could not be distinguished, except with some highly elastic polyacrylamide solutions where premature air entrainment due to hydrodynamic instability could be observed at speeds *lower* than V_{dwf} as will be detailed below. In order to reduce experimental errors, each data point was

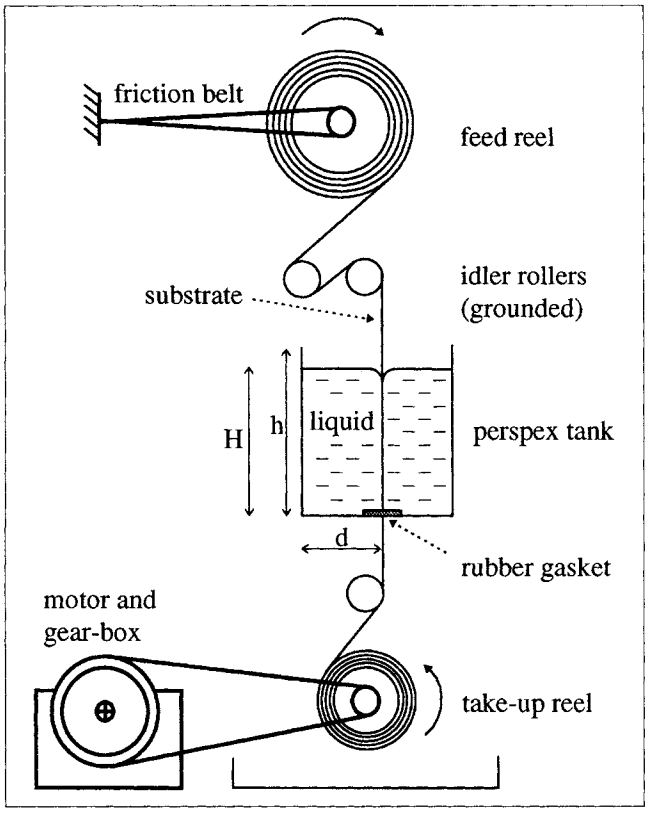

Figure 2. Experimental setup.

repeated at least five times. The relative standard deviation was always found to be lower than 3.5%, being even less than 2% in most cases. All coating experiments were conducted at room temperature (between 20 and 25°C), and the actual temperature of the liquid T_{exp} was carefully recorded (see Table 1).

Non-Newtonian coating liquids were made by dissolving small amounts of either polyacrylamide (PAA) or carboxymethyl cellulose (CMC)—both supplied by BDH, Poole, England—in 80% and 50% glycerin/water solutions (note that all concentrations in this article are given in weight). The molecular weight of the PAA was greater than 5×10^6 g/mol. The CMC sodium salt powder used was referred to as "high viscosity" by the supplier, and its molecular weight was around 7×10^5 g/mol. Stock solutions of 0.25% PAA and 0.5% CMC in water were first made and mixed thoroughly for several days. The test liquids were then prepared by mixing suitable quantities of stock solution, water, and glycerin. Each solution was mixed at low speed for 24 h with a propeller mixer and left to rest overnight prior to the coating experiments. With this standardized method of preparation, uncertainties resulting from undesirable effects such as absorption of air moisture by glycerin and shear-induced polymer degradation during mixing could be minimized. The stock solutions of 0.25% PAA and 0.5% CMC in water were also tested for completeness.

Rheology of Coating Solutions

The rheological properties (viscosity and first normal stress difference) of all coating solutions were measured in steady shear at 20°C ± 1 with a Sangamo R18 Weissenberg Rheogoniometer equipped with a cone-and-plate cell (cone angle: 1°; cell diameter: 10 cm). The raw data obtained when measuring the first normal stress difference at high shear rates were corrected to account for centrifugal effects (Whorlow, 1992). The validity of the correction formula was checked with the

Table 1. Physical Properties and Selected Rheological Parameters of All Tested Liquids at T_{exp} (except S_R Values at $T = 20°C \pm 1°$)

	T_{exp} (°C)	ρ (kg/m^3)	σ (mN/m)	μ_{400} (mPa·s)	μ_s (mPa·s)	S_R at 20°C 230 s^{-1}	S_R at 20°C 910 s^{-1}
80% Glycerin in water	24.7	1,206	63	51	51	—	—
PAA 50 ppm in 80% gly-water	23.9	1,207	62	59	53	0.4	0.9
— 100 ppm	25.2	1,204	64	51	49	1.0	2.0
— 250 ppm	24.2	1,205	63	85	52	1.9	4.6
— 375 ppm	24.8	1,205	63	96	50	5.8	10.8
— 500 ppm	21.9	1,207	63	104	59	8.6	> 20
CMC 100 ppm	24.6	1,207	64	62	51	—	0.3
— 250 ppm	23.8	1,206	64	84	53	0.7	0.8
— 500 ppm	24.0	1,208	60	100	52	1.2	1.4
— 1,000 ppm	24.8	1,208	65	132	50	1.8	1.9
50% Glycerin in water	22.7	1,124	64	6.5	6.5	—	—
PAA 25 ppm in 50% gly-water	21.2	1,125	66	7.6	6.8	—	—
— 50 ppm	21.6	1,124	67	8.5	6.7	—	—
— 100 ppm	22.7	1,124	66	9.5	6.5	—	3.5
— 250 ppm	22.4	1,124	67	12.2	6.5	2.1	4.7
— 500 ppm	22.4	1,124	66	14.7	6.5	3.0	5.7
CMC 50 ppm	21.3	1,125	66	8.5	6.8	—	—
— 100 ppm	21.6	1,125	67	9.7	6.7	—	—
— 250 ppm	21.0	1,125	66	14.0	6.9	—	1.3
— 500 ppm	21.6	1,125	68	21.3	6.7	1.0	1.6
— 1,000 ppm	22.2	1,125	68	34.5	6.6	1.8	2.3
PAA 0.25% in water	22.0	1,000	65	14	≈ 1	3.7	7.6
CMC 0.50% in water	22.3	1,000	70	55	≈ 1	1.4	2.1

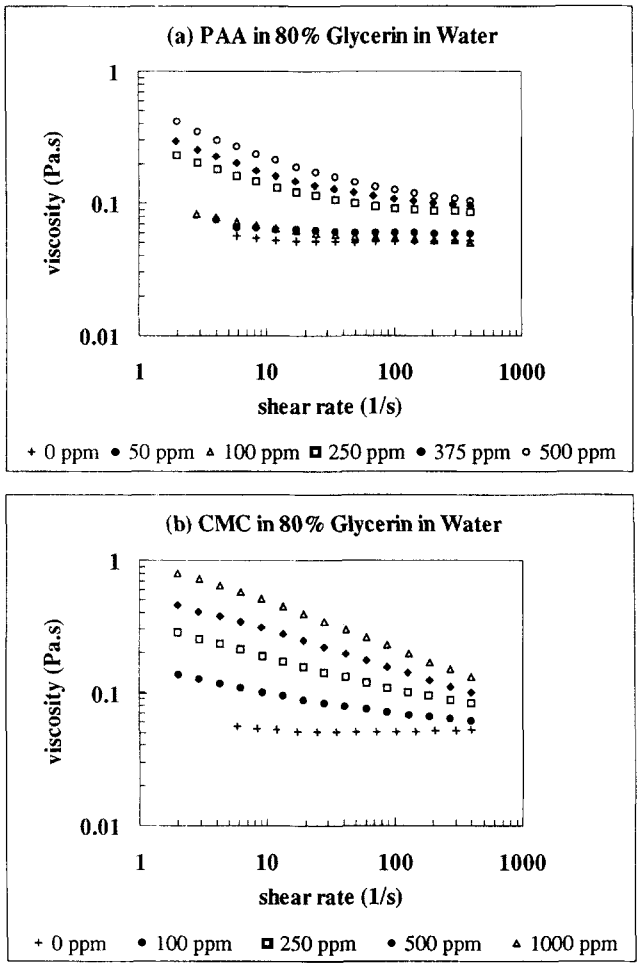

Figure 3. Viscosity functions at T_{exp} of (a) PAA and (b) CMC solutions in 80% glycerin in water (rheometer Carrimed CS100).

Newtonian 80% glycerin/water solution. Additional viscosity measurements were also carried out with a Carrimed CS100 controlled stress rheometer fitted with a cone-and-plate fixture (cone angle: 2°, cone diameter: 5 cm) and equipped with a Peltier system allowing an accurate control (within 0.1°C) of the sample temperature. For each liquid, the data obtained with this instrument were taken at the temperature T_{exp} recorded during the corresponding coating experiment. The surface tensions were also measured at $T_{exp} \pm 0.1$°C with a Krüss K10ST digital tensiometer using the Du Nouÿ ring method. For each liquid, air entrainment experiments, rheological characterizations and, whenever possible, surface tension measurements were carried out on the same day to minimize errors due to air-moisture absorption or polymer biodegradation.

The viscosity functions at T_{exp} of all tested liquids are shown in Figures 3 to 5. Selected rheological and physical parameters are also reported in Table 1. Although the viscosity of the most dilute PAA solutions (50 ppm in 80% and 25 ppm in 50% glycerin in water) may appear constant over the range of shear rates (2–400 s^{-1}) covered by our measurements, all polymer solutions present some degree of shear thinning over this range. Since the shear rates involved in the dynamic wetting process are likely to be quite high (Blake and Ruschak, 1997), the apparent viscosities of the polymer solutions at high shear rates are of prime interest. At extremely high shear rates, the viscosity function of any polymeric liquid reaches an upper Newtonian plateau of constant viscosity μ_∞ (Bird et al., 1987). The data suggest that this upper Newtonian plateau is practically reached at 400 s^{-1} for all PAA solutions in glycerin/water solvent (Figures 3a and 4a). At this shear rate, these solutions shear-thin only marginally (if at all), so that μ_∞ is close (if not equal) to the apparent viscosity of the solution at 400 s^{-1} (μ_{400}). The temperature dependence of the viscosity being set apart, μ_∞ increases with the polymer concentration (at constant glycerin concentration) and is higher than the viscosity μ_s of the glycerin/water solvent at the same temperature. Conversely, all CMC solutions and the 0.25% PAA solution in water remain strongly shear thinning at 400 s^{-1}, as shown in Figures 3b, 4b, and 5. Presumably, the upper Newtonian plateau with these solutions begins at shear-rate values of order of 10^3 to 10^5 s^{-1}. As a result, μ_∞ for any of these solutions remains unknown. It lies somewhere between the apparent viscosity

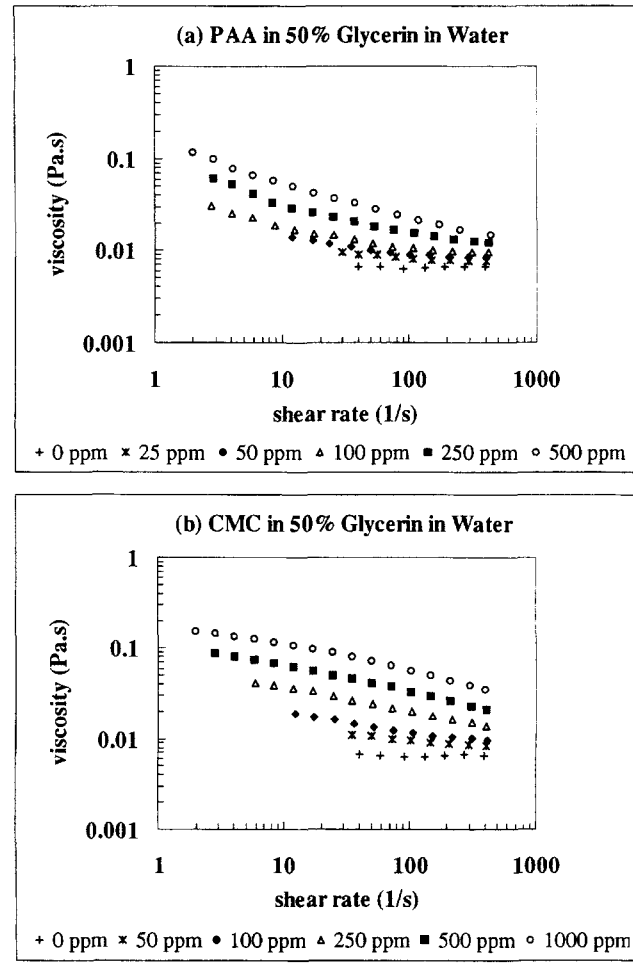

Figure 4. Viscosity functions at T_{exp} of (a) PAA and (b) CMC solutions in 50% glycerin in water (rheometer Carrimed CS100).

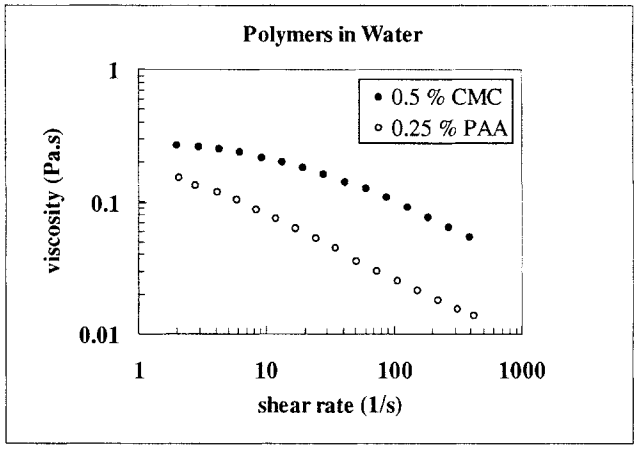

Figure 5. Viscosity functions at T_{exp} of PAA and CMC solutions in water (rheometer Carrimed CS100).

of the solution at 400 s^{-1}, μ_{400}, and the viscosity μ_s of the glycerin/water solvent (that is, $\mu_s < \mu_\infty < \mu_{400}$). Most probably, it also increases with the polymer concentration. For each polymer solution, numerical values of μ_s and μ_{400} measured at T_{exp} are reported in Table 1.

The elastic properties of the liquids are given by the recoverable shear, defined as (Middleman, 1977)

$$S_R = \frac{1}{2}\frac{\tau_{11} - \tau_{22}}{\tau_{12}} \tag{4}$$

where $\tau_{11} - \tau_{22}$ is the first normal difference and τ_{12} is the shear stress, at a given shear rate $\dot{\gamma}$. Values of S_R, as measured with the R18 Weissenberg Rheogoniometer at the shear rates of 230 and 910 s^{-1}, are reported in Table 1. As expected, the elasticity of the PAA solutions was found to be significantly greater than that of the CMC solutions (see Table 1). During mixing, the PAA solutions of concentration above 250 ppm in 80% glycerin in water exhibited the Weissenberg effect, or rod-climbing (Bird et al., 1987). This effect of elastic origin was never observed with any of the CMC solutions.

Results and Discussion

Air entrainment due to instability of bulk flow

With all PAA solutions of concentration higher than 100 or 250 ppm, the bulk flow in the tank was observed to be unstable at high substrate velocities. The instability manifested itself by the formation of cusps on the free surface of the liquid, as photographed in Figure 6. An important observation is that the cusps formed *gradually* as the speed was increased, that is, the instability does not seem to have a sharp onset. The cusps would first form near the wetting line and would extend over the whole liquid surface as the speed was increased. They would also travel slowly and randomly along the width of the substrate. As the speed was increased, the tips of the cusps in contact with the substrate were dragged deeper below the mean liquid level and ultimately would break up into large air bubbles that were entrained into the liquid. Clearly, this type of air entrainment was *independent* of the phenomenon of dynamic wetting failure described above. As the substrate speed was increased, dynamic wetting failure could be observed before, or after, the formation of cusps, depending on the PAA concentration. With the 500 ppm PAA solution in 80% glycerin/water solvent, air entrainment due to cusps formation occurred at substrate speeds as low as 12 cm/s, whereas dynamic wetting failure could only be observed at speeds above 36 cm/s. When the PAA concentration was reduced to 250 ppm in the same solvent, the speed at which cusps began to form was about 30% higher than V_{dwf}.

Since the cusp instability was never observed with any of the CMC solutions, it is reasonable to attribute it to elastic effects. In our experiments, it could be observed only for polymer solutions exhibiting a recoverable shear S_R greater than about 3 (see Table 1). Increased S_R also corresponded clearly to more unstable flows. Further investigations of the elastic instability of free-surface, side-driven cavity flows are needed to determine precisely the conditions at which it occurs. This problem certainly shares some common features with the elastic instability of a lid-driven cavity flow (with no free surface) recently observed by Pakdel et al. (1997). It may also have some links with elastic instabilities of other free-surface flows in coating operations that lead to coating defects such as "rough surface" in slot coating (Ning et al., 1996) or "mottle" in reverse roll coating (Coyle et al., 1990). The new finding of the present work is that such elastic instabilities can also lead to air entrainment.

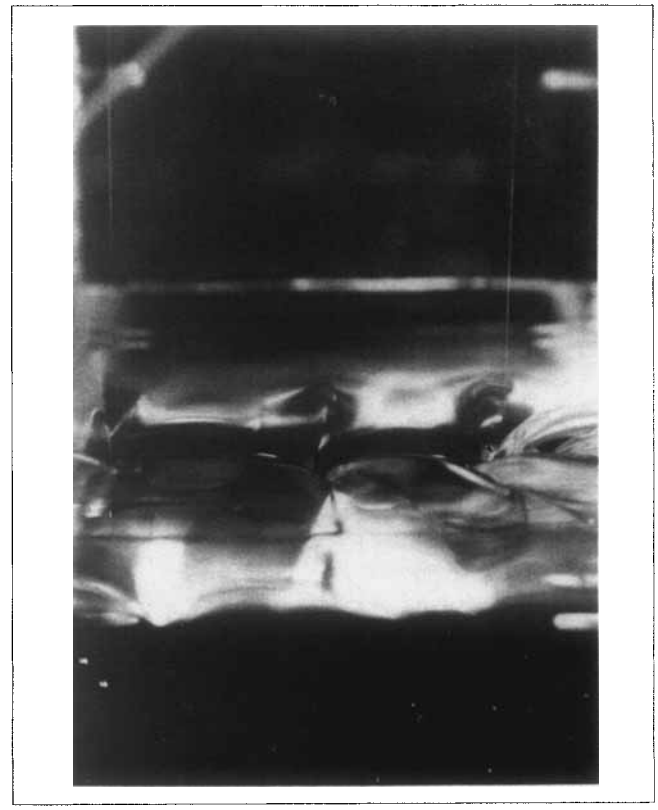

Figure 6. Formation of cusps on the liquid surface with the 500 ppm PAA solution in 80% glycerin in water ($V \approx 25$ cm/s).

Table 2. Experimental Results (V_{dwf}) and Comparison with Critical Velocities Calculated with Eq. 1 Using the Viscosities at 400 s^{-1} of the Polymer Solutions (V_{dwf}^{400}) and the Viscosities of the Newtonian Bases at T_{exp} (V_{dwf}^{s})

	Exp.	Calc. with Eq. 1	
	V_{dwf} (cm/s)	V_{dwf}^{400} (cm/s)	V_{dwf}^{s} (cm/s)
80% Glycerin in water	44	44	44
PAA 50 ppm in 80% gly-water	42	39	43
— 100 ppm	43	44	45
— 250 ppm	41	30	43
— 375 ppm	40	27	44
— 500 ppm	36	26	40
CMC 100 ppm	39	38	45
— 250 ppm	39	30	43
— 500 ppm	40	26	43
— 1,000 ppm	37	21	45
50% Glycerin in water	231	212	212
PAA 25 ppm in 50% gly-water	157	189	206
— 50 ppm	159	175	210
— 100 ppm	163	160	215
— 250 ppm	168	132	213
— 500 ppm	170	114	213
CMC 50 ppm	191	175	207
— 100 ppm	180	158	209
— 250 ppm	163	118	205
— 500 ppm	156	87	210
— 1,000 ppm	152	60	214
PAA 0.25% in water	$\gg 300$	114	≈ 800
CMC 0.50% in water	$\gg 300$	41	≈ 800

Dynamic wetting failure velocities

Whether or not elastic instabilities of the bulk flow occurred and caused detrimental air entrainment at speeds lower than V_{dwf}, the determination of the dynamic wetting failure velocity is important as this provides information about the physics of wetting at the three-phase contact line. The results obtained are all reported in Table 2. Depending on the liquids used, measured velocities for dynamic wetting failure ranged from 36 cm/s to more than 2 m/s. The critical speeds for both polymer solutions in water (0.25% PAA and 0.5% CMC) were higher than the maximum speed of our experimental coater (3 m/s) and, hence, could not be determined.

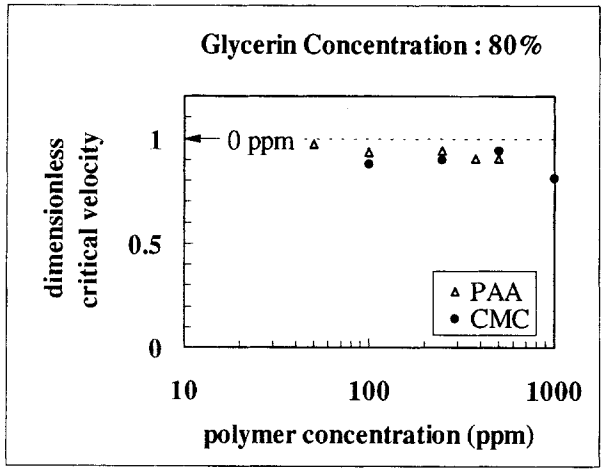

Figure 7. Dimensionless dynamic wetting failure velocity V_{dwf}/V_{dwf}^{s} as a function of the polymer concentration for PAA and CMC solutions in 80% glycerin/water solvent.

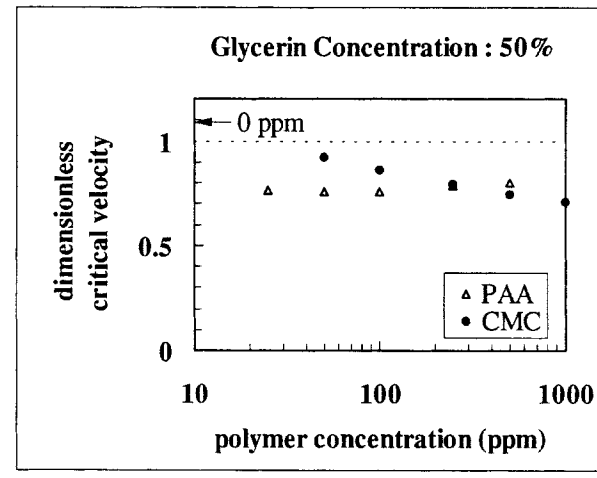

Figure 8. Dimensionless dynamic wetting failure velocity V_{dwf}/V_{dwf}^{s} as a function of the polymer concentration for PAA and CMC solutions in 50% glycerin/water solvent.

With both Newtonian solutions of glycerin 80% and 50% in water, the measured dynamic wetting failure velocities compare very well with the predictions of Eq. 1. The agreement is excellent with the 80% glycerin solution. With the 50% glycerin solution, the experimentally measured critical velocity exceeds the predicted one by about 9%, but it should be recalled that the viscosity of this solution (6.5 mPa·s) falls outside the range for which Eq. 1 is fully valid (see Burley and Jolly, 1984). When small quantities of either PAA (up to 500 ppm) or CMC (up to 1,000 ppm) are added to these solutions, the dynamic wetting failure velocity V_{dwf} is only affected marginally and tends to decrease, as shown in Table 2. However, while small variations of surface tension and density from one liquid to another (at the same glycerin concentration) are negligible, the raw V_{dwf} data in Table 2 actually include the effect of viscosity variations with temperature, as all data points were not taken exactly at the same temperature (see Table 1). In order to remove this artifact, the data are better plotted as in Figures 7 and 8. Here, the measured critical velocities are made dimensionless with the critical velocities V_{dwf}^{s} of the Newtonian glycerin/water solvents, calculated for each data point using Eq. 1 and the solvent viscosity μ_s *measured at the temperature* T_{exp} *recorded during the corresponding coating experiment (Table 1).*

Thus, Figures 7 and 8 show the true effect of PAA or CMC additives on the dynamic wetting failure velocity. Based on the findings of Bolton and Middleman (1980) on air entrainment at a liquid/liquid juncture, it was hoped that dynamic wetting failure could be delayed substantially by adding small amounts of polymer to the Newtonian base. Unfortunately, the results show that this is not the case. The critical velocities of polymer solutions were all lower than those of the Newtonian bases. In the 80% glycerin/water solvent, however, they were all confined within 20% of the dynamic wet-

ting failure velocity of the Newtonian base (Figure 7). As will be discussed later, this is remarkable when one considers the large discrepancies in the viscosity of these solutions (see Figure 3). The results obtained in the 50% glycerin/water solvent are even more surprising. In this solvent (Figure 8), the dynamic wetting failure velocity decreases steadily with the CMC concentration, which *might* be attributed to the corresponding increase in viscosity (see below). However, it is not very sensitive to (or even *increases* with) the PAA concentration in the range 25–500 ppm, in spite of substantial viscosity variations (Figure 4a). Additionally, the nearly constant critical velocity over this range of PAA concentration, 1.63 ± 0.07 m/s, is significantly lower than that of the glycerin/water solvent (2.31 m/s). These latter data were not erroneous and was replicated with a newly made 50% glycerin/water solution.

Correlation with viscosities

As mentioned above, Eq. 1 provides reliable predictions of V_{dwf} for Newtonian liquids that are extremely useful from an engineering viewpoint. In this section, its possible generalization to non-Newtonian liquids is examined. Since both densities and surface tension variations with polymer concentrations were found to be negligible (Table 1), the discussion focuses only on the viscosity dependence of V_{dwf}. With polymer solutions, however, the value of the apparent viscosity to enter Eq. 1 is difficult to establish as the shear rate at which it should be measured is not known. We chose arbitrarily to consider the apparent viscosities at 400 s^{-1} (μ_{400}), that is, at the highest shear rate covered by our measurements. This enables us to define V_{dwf}^{400} as the critical velocity calculated using Eq. 1 and μ_{400}. At shear rates below 400 s^{-1}, the apparent viscosity of any polymer solution is greater than μ_{400} and if entered in Eq. 1 would yield a velocity *lower* than V_{dwf}^{400}. Conversely, the viscosity of any PAA solutions in either glycerin/water solvent at shear rates above 400 s^{-1} is close to μ_{400}, hence Eq. 1 cannot yield velocities much greater than V_{dwf}^{400} with these solutions.

Values of V_{dwf}^{400} calculated with the physical properties of the liquids measured at T_{exp} are reported in Table 2 and compared with the experimentally measured dynamic wetting failure velocities V_{dwf}. In most cases, V_{dwf}^{400} is lower than V_{dwf}, especially for the most shear-thinning solutions. The discrepancy may be very large, as for instance with the 0.5% CMC solution in water where V_{dwf}^{400} and V_{dwf} are 0.41 and more than 3 m/s, respectively. In other words, predictions based on Eq. 1 and the apparent viscosity of the liquid at $\dot{\gamma} \leq 400$ s^{-1} usually underestimate, sometimes very much, the dynamic wetting failure velocity of shear-thinning liquids. Therefore, if the basis of comparison is the viscosity of the liquids *within the easily measurable range of shear rates* (below, say, 400 s^{-1}), dynamic wetting failure occurs with shear-thinning liquids at speeds higher than Newtonian liquids of comparable viscosity. This result is consistent with the limited observations reported by Gutoff and Kendrick (1982, 1987) and Blake and Ruschak (1997). It also agrees qualitatively with the conclusions of Ghannam and Esmail (1997), at least with our polymer solutions in 80% glycerin in water for which the characteristic shear rate, as established with Eqs. 2 to 3, was always lower than 400 s^{-1}.

In most cases, thus, the experimental critical velocity V_{dwf} is such that $V_{dwf}^{400} < V_{dwf} < V_{dwf}^{s}$. It is then tempting to assume that V_{dwf} is determined by the liquid apparent viscosity $\mu_+ < \mu_{400}$ at a certain (unknown) shear rate above 400 s^{-1}. With power-law fluids such as CMC solutions (Figures 3b and 4b), it may be estimated from the data that this shear rate would be of the order of 3×10^3 to 2×10^4 s^{-1}. However, the above assumption does not hold with PAA solutions of concentration higher than 250 ppm for which μ_+ cannot be sufficiently lower than μ_{400} (Figures 3a and 4a). Additionally, it cannot explain why the critical velocity V_{dwf} of PAA solutions in 50% glycerin/water solvent is practically constant or even *increases* with the polymer concentration in the wide range 25–500 ppm (Figure 8). It cannot also account for the drop in V_{dwf} observed when the PAA concentration in this solvent was increased from 0 to 25 ppm, with very little change on the viscosity.

There is no evidence that these unexpected results obtained with PAA solutions in 50% glycerin in water could be attributed to the liquid elasticity. With PAA solutions of concentration less than 250 ppm in the 80% glycerin/water solvent, V_{dwf}^{400} correlates well with V_{dwf} although these solutions exhibited measurable normal stresses. Conversely, with relatively inelastic CMC solutions in the same solvent (Figure 7), V_{dwf} also appears little dependent on the polymer concentration between 100 and 1,000 ppm. Overall, the data suggest that dynamic wetting failure velocities with polymer solutions do not correlate very well with readily measurable rheological properties. In particular, any attempt to generalize Eq. 1 using the liquid apparent viscosity at a particular shear rate is bound to fail. Perhaps, the most striking result of our study is that the best estimate of the critical velocity of any of our polymer solutions is in fact provided by V_{dwf}^{s}, that is, the dynamic wetting failure velocity calculated using Eq. 1 and the *viscosity of the Newtonian solvent* μ_s. Indeed, V_{dwf} was no lower than 0.75 V_{dwf}^{s} in all cases but one (see Table 2).

Discussion

In the absence of a universally accepted theory of the physics of forced dynamic wetting with Newtonian liquids (let alone the critical and complex phenomena of dynamic wetting failure and contact line instability), interpreting the above results is difficult. Nevertheless, a few remarks may be formulated. To begin with, there is considerable evidence that the critical speed for dynamic wetting failure usually depends on the bulk flow of the liquid near the wetting line (Perry, 1967; Blake et al., 1994; Veverka, 1995). In our experiments, altering the liquid rheology probably affected the flow field in the tank and, therefore, this argument might be invoked to explain our data. However, experimental observations show that such an explanation is inadequate or at least incomplete. The work of Pakdel et al. (1997) on lid-driven cavity flows suggests that the flow in the tank is sensitive to both the aspect ratio of the cavity a_c and the fluid elasticity. In spite of this, critical velocities were not found to be noticeably affected by changes in a_c in the range 0.6–1.6, and no clear evidence of any elastic effects on V_{dwf} was obtained. Additionally, whether or not the elastic instability (described in the subsection on air entrainment due to instability of bulk flow) occurred did not seem to affect the dynamic wetting

failure velocity. In summary, bulk flow phenomena did not interfere with the dynamic wetting process in our experiments. Therefore, our experimental results cannot be explained simply by the effect of fluid rheology on the macroscopic hydrodynamics near the wetting line.

On the other hand, events occurring at the microscopic scale at or very close to the dynamic wetting line are worth considering. Dynamic wetting has been modeled as an adsorption/desorption process in which, as the wetting line advances, molecules of air adsorbed on the solid are displaced by molecules from the advancing liquid (Blake and Haynes, 1969; Blake, 1993). This model provides a physical explanation for the existence of a maximum speed of wetting. In the simplest case (Blake and Haynes, 1969), molecular interactions between the liquid and the solid are the main hindrance to the motion of the wetting line. However, viscous interactions also retard molecular displacement (Cherry and Holmes, 1969), and this effect was incorporated by Blake (1993) in a combined theory. In contrast to hydrodynamic models of dynamic wetting such as Cox (1986), a *nonhydrodynamic* contribution of viscosity on the maximum wetting speed V_{dwf} results from this approach. Since rheology only refers to macroscopic hydrodynamics, this could explain the experimental finding that dynamic wetting failure velocities with polymer solutions hardly correlate with fluid rheology. Inversely, the experimental results obtained throughout the present study suggest that dynamic wetting is dominated by events occurring at the microscopic scale close to the wetting line and cannot be modeled using hydrodynamic arguments only. At the molecular level, polymer solutions cannot be viewed as homogeneous liquids. That the dynamic wetting failure velocities of our polymer solutions were close to those obtained with the corresponding Newtonian bases may therefore be interpreted by considering that long chain molecules do not participate much to the wetting process which involves mainly the small molecules of the solvent.

The importance of nonhydrodynamic interactions at the contact line has been also pointed out by Shikhmurzaev (1993). He showed that the system of dimensionless similarity parameters used in classical hydrodynamic models—where the liquid is characterized only by its viscosity, surface tension, and density—is *not* complete. This may explain, for instance, that Eq. 1 cannot be expressed in the dimensionless form. To describe the liquid flow in the immediate vicinity of the contact line, additional parameters, such as surface tension relaxation time, slip coefficient, and so on, must be introduced. We do not know how these additional parameters behave with polymer solutions. Until this is clarified, the dynamic wetting failure velocity of a given polymer solution can therefore only be obtained from experimental measurements.

Summary and Conclusions

An experimental investigation of the effect of fluid rheology on the air entrainment velocity in plunging tape experiments with smooth plastic substrates has been carried out. Dilute PAA and CMC solutions in Newtonian glycerin/water solvents have been used as test fluids. It was found that fluid elasticity gives rise to flow instabilities that may lead to air entrainment. In such case, the air entrainment mechanism is purely hydrodynamic and is independent of the phenomenon of dynamic wetting. Regardless whether or not this occurred, the critical velocity for dynamic wetting failure was measured with all the solutions. It was found that although small additions of polymer affect the rheological properties of glycerin/water solutions significantly, the critical velocities for dynamic wetting failure are relatively little affected. The results show that the critical velocity of a given non-Newtonian liquid cannot be accurately predicted from readily measurable rheological data. It may, however, be estimated roughly from the critical velocity of the Newtonian solvent of the polymer solution. Estimates based on correlations for Newtonian liquids using the viscosity of the solutions at the upper Newtonian plateau (when measurable) did not prove more accurate.

Unlike in most coating flows, the dynamic wetting process in plunging tape experiments is little affected by the macroscopic hydrodynamics near the wetting line (Blake and Ruschak, 1997). As a result, the effect of fluid rheology on the dynamic wetting failure velocity cannot be explained simply by changes in the flow field near the wetting line. Conversely, the results suggest that the dynamic wetting failure velocity is determined by nonhydrodynamic interactions at the molecular scale where the very concept of rheology ceases to have a meaning.

Acknowledgments

This work was supported by a Marie Curie fellowship awarded to Dr. Cohu under the Training and Mobility of Researchers Programme of the Commission of European Communities. The authors would like to thank Dr. W. C. MacSporran for fruitful discussions.

Literature Cited

Bird, R. B., R. C. Armstrong, and O. Hassager, *Dynamics of Polymeric Liquids: 1. Fluid Mechanics*, 2nd ed., Wiley Interscience, New York (1987).

Blake, T. D., "Dynamic Contact Angles and Wetting Kinetics," *Wettability, Surfactant Science Series*, Vol. 49, J. Berg, ed., Marcel Dekker, New York, p. 2367 (1993).

Blake, T. D., A. Clarke, and K. J. Ruschak, "Hydrodynamic Assist of Dynamic Wetting," *AIChE J.*, **40**, 229 (1994).

Blake, T. D., and J. M. Haynes, "Kinetics of Liquid/Liquid Displacement," *J. Colloid Interf. Sci.*, **30**, 421 (1969).

Blake, T. D., and K. J. Ruschak, "A Maximum Speed of Wetting," *Nature*, **282**, 489 (1979).

Blake, T. D., and K. J. Ruschak, "Wetting: Static and Dynamic Contact Lines," in *Liquid Film Coating: Scientific Principles and their Technological Implications*, S. F. Kistler and P. M. Schweitzer, eds., Chapman and Hall, London, p. 63 (1997).

Bolton, B., and S. Middleman, "Air Entrainment in a Roll Coating System," *Chem. Eng. Sci.*, **35**, 597 (1980).

Buonopane, R. A., E. B. Gutoff, and M. M. T. Rimore, "Effect of Plunging Tape Surface Properties on Air Entrainment Velocity," *AIChE J.*, **32**, 682 (1986).

Burley, R., "Air Entrainment and the Limits of Coatability," *JOCCA*, **75**, 192 (1992).

Burley, R., and B. S. Kennedy, "An Experimental Study of Air Entrainment at a Solid-Liquid-Gas Interface," *Chem. Eng. Sci.*, **31**, 901 (1976).

Burley, R., and R. P. S. Jolly, "Entrainment of Air into Liquids by a High Speed Continuous Solid Surface," *Chem. Eng. Sci.*, **39**, 1357 (1984).

Cherry, B. W., and C. M. Holmes, "Kinetics of Wetting of Surfaces by Polymers," *J. Colloid Interf. Sci.*, **29**, 174 (1969).

Cohu, O., and H. Benkreira, "Air Entrainment in Angled Dip Coating," *Chem. Eng. Sci.*, **53**, 533 (1998).

Cox, R. G., "The Dynamics of the Spreading of Liquids on a Solid Surface. Part 1. Viscous Flow," *J. Fluid Mech.*, **168**, 169 (1986).
Coyle, D. J., C. W. Macosko, and L. E. Scriven, "Reverse Roll Coating of Non-Newtonian Liquids," *J. Rheol.*, **34**, 615 (1990).
Deryagin, B. M., and S. M. Levi, *Film Coating Theory*, Focal Press, London (1964).
Ghannam, M. T., and M. N. Esmail, "Experimental Study on Wetting of Fibers with Non-Newtonian Liquids," *AIChE J.*, **43**, 1579 (1997).
Gutoff, E. B., and C. E. Kendrick, "Dynamic Contact Angles," *AIChE J.*, **28**, 459 (1982).
Gutoff, E. B., and C. E. Kendrick, "Low-Flow Limit of Coatability on a Slide Coater," *AIChE J.*, **33**, 141 (1987).
Middleman, S., *Fundamentals of Polymer Processing*, McGraw-Hill, New York (1977).
Ning, C. Y., C. C. Tsai, and T. J. Liu, "The Effect of Polymer Additives on Extrusion Slot Coating," *Chem. Eng. Sci.*, **51**, 3289 (1996).
O'Connell, A., "Observation of Air Entrainment and the Limits of Coatability," PhD Thesis, Heriot-Watt Univ., Edinburgh, Scotland (1989).
Pakdel, P., S. H. Spiegelberg, and G. H. McKinley, "Cavity Flows of Elastic Liquids: Two-Dimensional Flows," *Phys. Fluids*, **9**, 3123 (1997).
Perry, R. T., "Fluid Mechanics of Entrainment through Liquid-Liquid and Liquid-Solid Junctures," PhD Thesis, University of Minnesota (1967).
Severtson, Y. C., and C. K. Aidun, "Stability of Two-Layer Stratified Flow in Inclined Channels: Application to Air Entrainment in Coating Systems," *J. Fluid Mech.*, **312**, 173 (1996).
Shikhmurzaev, Y. D., "The Moving Contact Line on a Smooth Solid Surface," *Int. J. Multiphase Flow*, **19**, 589 (1993).
Veverka, P. J., "An Investigation of Interfacial Instability during Air Entrainment," PhD Thesis, Inst. of Paper Science and Technol., Atlanta (1995).
Veverka, P. J., and C. K. Aidun, "Dynamics of Air Entrainment at the Contact Line," *J. Fluid Mech.*, in press (1998).
Whorlow, R. W., *Rheological Techniques*, 2nd ed., Ellis Horwood, New York (1992).

Manuscript received May 4, 1998, and revision received Aug. 5, 1998.